

# Dynamics of an Inverted Pendulum with Horizontal Sinusoidal Actuation

Kaden Cassidy

December 10, 2023

## 1 Introduction

We consider an inverted pendulum of length  $\ell$  and mass  $m$ , constrained to pivot about a point that moves horizontally. Gravity acts in the negative  $y$ -direction. We define the angle  $\theta$  so that  $\theta = 0$  corresponds to the pendulum pointing straight up along the positive  $y$ -axis. The pivot is driven horizontally according to

$$x_{\text{pivot}}(t) = x_0 \sin(\omega t), \quad y_{\text{pivot}} = 0,$$

where  $x_0$  is the horizontal oscillation amplitude and  $\omega$  is a constant angular frequency.

Unlike the standard pendulum, this system can exhibit a rich variety of behaviors, including stable oscillations about the inverted position for sufficiently strong and fast driving. Our goal is to derive the equations of motion using the Lagrangian formalism and then study the system under varying initial conditions.

## 2 Derivation of the Equations of Motion

### 2.1 Kinematics and Lagrangian

The position of the pendulum bob is given by

$$x(t) = x_0 \sin(\omega t) + \ell \sin \theta, \quad y(t) = \ell \cos \theta. \quad (1)$$

Note that  $y_{\text{pivot}} = 0$ , and we have chosen the vertical axis  $y$  positive upwards, with  $\theta = 0$  pointing straight up.

The velocities are:

$$\dot{x}(t) = \omega x_0 \cos(\omega t) + \ell \cos \theta \dot{\theta}, \quad (2)$$

$$\dot{y}(t) = -\ell \sin \theta \dot{\theta}. \quad (3)$$

The kinetic energy is

$$T = \frac{1}{2}m(\dot{x}^2 + \dot{y}^2) = \frac{m}{2} \left[ (\omega x_0 \cos(\omega t) + \ell \cos \theta \dot{\theta})^2 + (\ell \sin \theta \dot{\theta})^2 \right]. \quad (4)$$

Since  $\sin^2 \theta + \cos^2 \theta = 1$ , this can be expanded and rearranged, but we will keep it in this form for clarity.

The potential energy, with  $U = 0$  at  $y = 0$ , is

$$U = mgy = mg(\ell \cos \theta). \quad (5)$$

Hence, the Lagrangian is

$$L = T - U = \frac{m}{2} \left[ \omega^2 x_0^2 \cos^2(\omega t) + 2\omega x_0 \ell \cos(\omega t) \cos \theta \dot{\theta} + \ell^2 \dot{\theta}^2 \right] - mg\ell \cos \theta. \quad (6)$$

## 2.2 Non-Dimensionalizing Variables: $\tau$ and $\lambda$

To simplify the analysis, we introduce dimensionless variables. First, let us non-dimensionalize time by defining

$$\tau = \omega t.$$

Then

$$t = \frac{\tau}{\omega}$$

and

$$\frac{d\tau}{dt} = \omega.$$

We also define  $\lambda$  to non-dimensionalize the initial parameter  $x_0$  further simplifying the final equation of motion

$$\lambda = \frac{x_0}{\ell}.$$

$\implies$

$$x_0 = \lambda \ell$$

Substituting in these two variables to the Lagrangian yeilds the new equtions

$$L = \frac{m\ell^2}{2} \left[ \omega^2 \lambda^2 \cos^2(\tau) + 2\omega \lambda \cos(\tau) \cos \theta \dot{\theta} + \dot{\theta}^2 \right] - mg\ell \cos \theta. \quad (7)$$

## 2.3 Euler-Lagrange Equations

The Euler-Lagrange equation for  $\theta$  is:

$$\frac{d}{dt} \left( \frac{\partial L}{\partial \dot{\theta}} \right) = \frac{\partial L}{\partial \theta}.$$

Solving each side yields

$$\frac{\partial L}{\partial \dot{\theta}} = m\ell^2 [\omega \lambda \cos \tau \cos \theta + \dot{\theta}].$$

$$\implies \frac{d}{dt} \left[ \frac{\partial L}{\partial \dot{\theta}} \right] = m\ell^2 \left[ \frac{d}{dt} (\omega \lambda \cos \tau \cos \theta) + \frac{d}{dt} (\dot{\theta}) \right].$$

$$= m2[\ddot{\theta}\omega^2\lambda \sin \tau \cos \omega \lambda \cos \tau \sin \theta \dot{\theta}].$$

and

$$\frac{\partial L}{\partial \theta} = m\ell^2\omega\lambda \cos \tau \sin \theta \dot{\theta} + mg\ell \sin \theta.$$

Setting these two equations equal and simplifying results in the differential equation below:

$$\ddot{\theta} = \sin(\theta) \left[ \left( \frac{g}{\ell} - \dot{\theta} \omega \lambda \cos(\tau) \right) + \omega \lambda (\omega \cos(\theta) \sin(\tau) + \cos(\tau) \sin(\theta)) \right].$$

This ODE can then be integrated numerically for given initial conditions and parameters.

By adjusting the parameters, we can explore the dynamics of the pendulum for chaos and other unexpected behaviors.

### 3 Computational Findings

During exploration of the system through numerical integration, surfaces of section were used as the main exploratory tool. Plots were made taking points in time where  $\tau \in \mathbb{Z}$ . A set of 500 points were used in most plots to benefit from shorter computation time while patterns were still recognizable.

Parameters  $\lambda$ ,  $\omega$  as well as  $\dot{\theta}_0$  and  $\theta_0$  were varied, results and conclusions are organized below.

#### 3.1 Varying $\dot{\theta}_0$

The most interesting results ended up being under varying initial conditions for  $\dot{\theta}$ . During testing, chaos was found, but the barriers before chaos exhibited unique behavior to the other initial conditions. The plots in Figure 1 and 2 below depict surfaces of section in these boundary regions between oval stability and chaos.

Using visualization software of these points, animations can be made that make understanding the data in time much more intuitive. From these animations, we noticed a pulsating motion in these boundary regions where the pendulum oscillates within smaller ranges first, then larger ranges, then returning to smaller ranges. This suggests the existence of normal modes across two frequencies of oscillation.

Conducting these visualization tests up until the boundary reveals that chaos is exhibited once these pulsating motions are great enough to break circa 0.82 radians outside of hanging vertical ( $\theta = \pi$ ) for  $\omega = 2$  and  $\lambda = 1$ . Interestingly, the pendulum exits this angle range when  $\dot{\theta}_0$  becomes too large as well as too small, which seems counterintuitive.

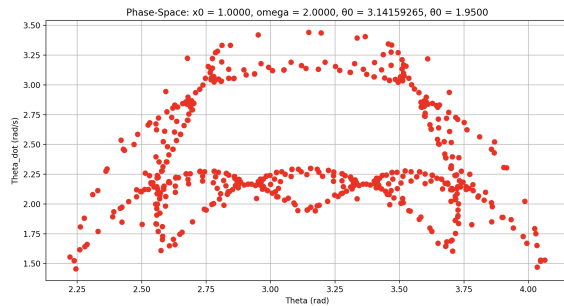


Figure 1: Boundary Region 1

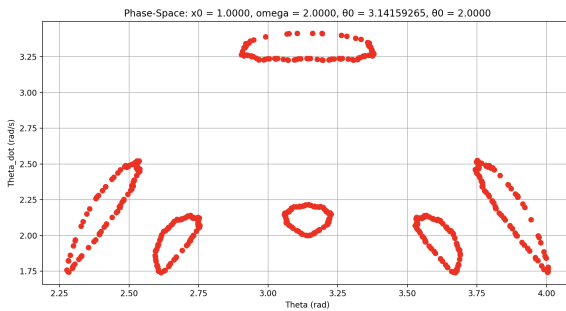


Figure 2: Boundary Region 2

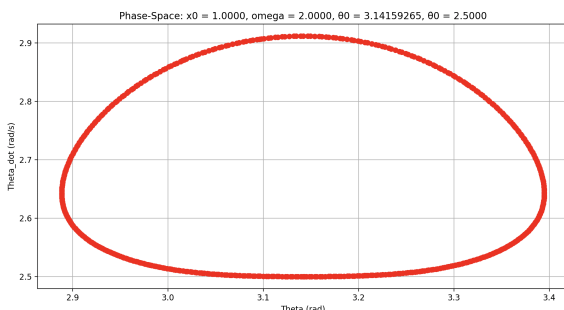


Figure 3: "Ovular Stability"

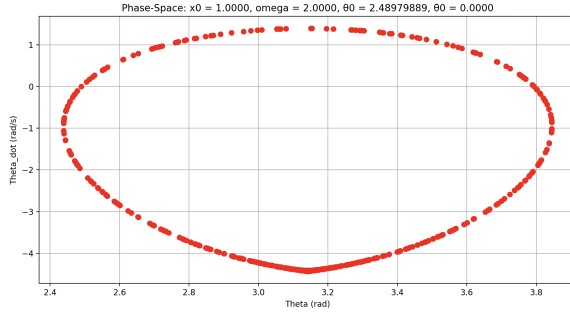


Figure 4: Stable Region

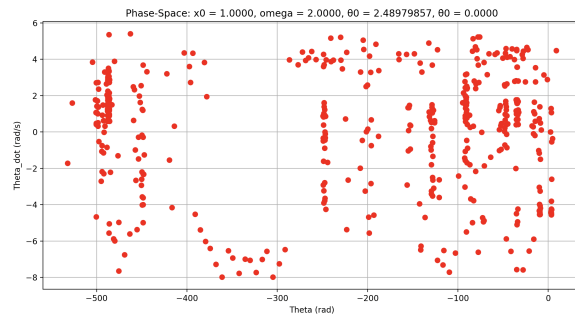


Figure 5: Unstable Region

It should also be noted that the only location  $\dot{\theta}$  appears in the equation of motion is where multiplied by  $\lambda$  and  $\omega$  suggesting a strong relation of these parameters to the angle range of stability that has not yet been explored.

### 3.2 Varying $\lambda$ , $\omega$ and $\theta_0$

$\lambda$  and  $\omega$  were varied significantly and produced very different shaped surfaces of section plots with a common theme: a fixed boundary  $\theta_0$  outside of which chaos was experienced. Similarly to the experimentation with  $\dot{\theta}_0$ , these boundaries of stability had an upper and lower bound, but unlike  $\dot{\theta}_0$ , no boundary regions exist. For example, plots in Figures 4 and 5 above have a difference in  $\theta_0$  of less than 0.000001 radians yet exhibit wildly different behavior.

Yet, some regions were found for other initial conditions of  $\lambda$  and  $\omega$  that when visualized with animation software depicted short lived stability that then devolved into chaos, the surface of section for that model is in Figure 6.

Other uniquely shaped surfaces of section were found, but did not demonstrate any unique behavior outside of their plots. These plots are included below alongside initial conditions in case further exploration is desired.

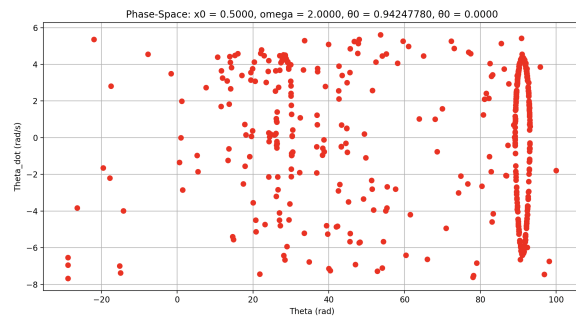


Figure 6: Short Lived Stability

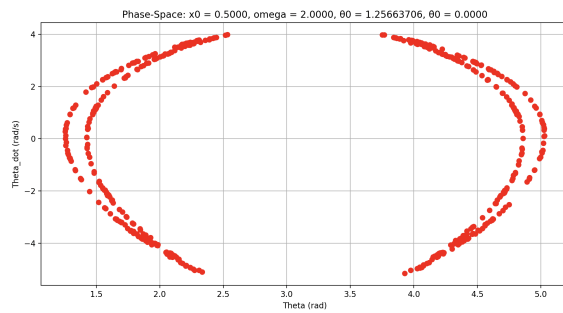


Figure 7:  $\lambda = 0.5, \omega = 2, \theta_0 = 1.2566$

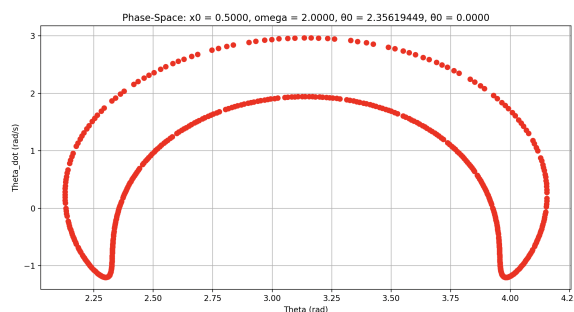


Figure 8:  $\lambda = 0.5, \omega = 2, \theta_0 = 2.356194$

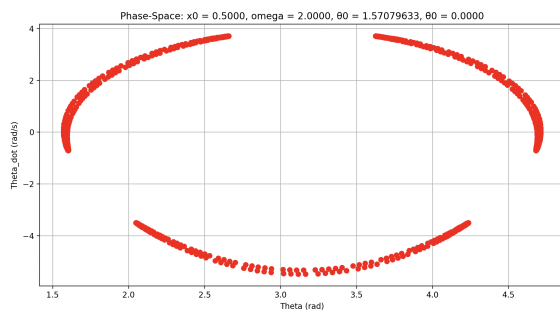


Figure 9:  $\lambda = 0.5, \omega = 2, \theta_0 = 1.570796$

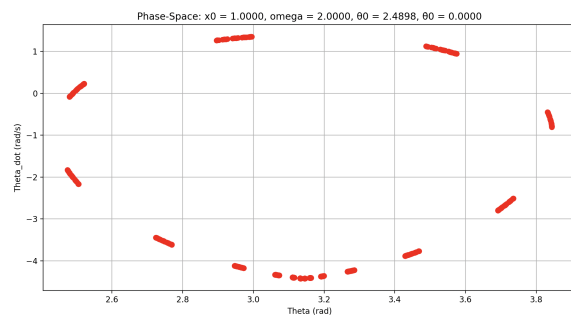


Figure 10:  $\lambda = 1, \omega = 2, \theta_0 = 2.4898$